AIP | Applied Physics Letters

Ordering-induced changes in the optical spectra of semiconductor alloys

J. E. Bernard, S.-H. Wei, D. M. Wood, and Alex Zunger

Citation: Applied Physics Letters **52**, 311 (1988); doi: 10.1063/1.99503
View online: http://dx.doi.org/10.1063/1.99503
View Table of Contents: http://scitation.aip.org/content/aip/journal/apl/52/4?ver=pdfcov
Published by the AIP Publishing

Ordering-induced changes in the optical spectra of semiconductor alloys

J. E. Bernard, S.-H. Wei, D. M. Wood, and Alex Zunger
Solar Energy Research Institute, Golden, Colorado 80401

(Received 24 April 1987; accepted for publication 17 November 1987)

It is shown how the recently predicted and subsequently observed spontaneous long-range ordering of pseudobinary $A_{0.5}B_{0.5}C$ isovalent semiconductor alloys into the $(AC)_1(BC)_1$ superlattice structure (a CuAuI-type crystal) gives rise to characteristic changes in the optical and photoemission spectra. We predict new direct transitions and substantial splittings of transitions absent in the disordered alloy.

The traditional viewpoint on the structure of isovalent semiconductor alloys $A_xB_{1-x}C$ has been that the mixed atoms A and B are invariably *disordered* on the same sublattice at all temperatures and compositions where solid solutions exist.[1-3] While this "universality" thought[1-3] to underlie all isovalent semiconductor alloys[1-3] contrasts with the great structural diversity exhibited by metal alloys (where both disordered and spontaneously *ordered* intermetallic phases frequently occur), it was nevertheless consistent with the absence of new diffraction spots (forbidden in the constituents AC and BC) in melt-grown semiconductor alloys,[1,2] with the smooth concentration and temperature variation of many alloy properties[3] (e.g., band gaps), and with the existence of *positive* excess mixing enthalpies at high temperatures for all such isovalent alloys.[1]

In violation of this basic paradigm, we have predicted theoretically[4] that at sufficiently low temperatures isovalent semiconductor alloys can exhibit either stable or metastable *long-range ordering* of compoundlike $A_nB_{4-n}C_4$ structures ($n = 1,2,3$), including for $n = 2$ the chalcopyrite ($I\bar{4}2d$) and CuAuI-like ($P\bar{4}m2$) structures, or the Cu_3Au-like ($P\bar{4}3m$) and Famatinite ($I\bar{4}2m$) structures for $n = 1$ and 3. These predictions seem to have been confirmed by recent direct observation of *spontaneously ordered phases*, grown on lattice-matched substrates (i.e., not strained-layer systems) with their attendant new diffraction patterns. These include $InGa_3As_4$ and In_3GaAs_4 (Ref. 5) (Famatinite or CuAuI-like phase), $InGaAs_2$ [Ref.6(a)] (CuAuI-like phase), Ga_2AsSb (Ref. 7) (chalcopyrite and CuAuI-like phases), and $InGaP_2$ (Ref. 8), $GaAlAs_2$ (Ref. 9) (CuAuI-like phase), and rhombohedral [Ref. 6(b)] $InGaAs_2$. Long-range order in these systems has been established by diffraction experiments. Here we show, using both group-theoretical arguments and self-consistent electronic structure calculations on eight ordered ABC_2 semiconductors, how the *optical* properties of CuAuI-like ordered phases differ from those of the binary constituents.

We first outline the basic physical ideas surrounding the evolution of band states of ordered ABC_2 from those of the disordered $A_{0.5}B_{0.5}C$ alloy. Imagine first the disordered alloy $A_{0.5}B_{0.5}C$ as a virtual crystal having the zinc-blende (ZB) crystal structure, a crystal potential $V_{ZB}(\mathbf{r})$ representing the concentration-weighted average of its constituents, and a zinc-blende-like band structure whose states we denote as $\tilde{\Gamma}, \tilde{X}, \tilde{L}$, etc. The common C atom has four identical (average) neighbors $\langle AB \rangle$, at equal distances $R = (\sqrt{3}/4)a$, where a is the average lattice parameter. On the other hand, the ordered tetragonal (T) structure ABC_2 [equivalent to an alternate monolayer superlattice $(AC)_1(BC)_1$ in the (001) direction[4] (see inset to Fig. 1) has a crystal potential $V_T(\mathbf{r})$ with different amplitudes on sites A and B, and band states at high symmetry points, which we denote by $\bar{\Gamma}, \bar{M}, \bar{R}$, etc. In this ordered ABC_2 structure, each C atom is coordinated by two A and two B atoms. Because in general the bond lengths R_{AC} and R_{BC} are unequal,[4] the C-atom displacement parameter $u = \frac{1}{4} + (R_{AC}^2 - R_{BC}^2)/\eta^2a^2$ and the tetragonal ratio $\eta = c/a$ may differ from the unrelaxed zinc-blende values (or those of the virtual alloy), where $R_{AC} = R_{BC}$, $u = \frac{1}{4}$, and $\eta = 1$. We now describe the evolution of the band structure of ordered ABC_2 in the CuAuI-like structure from that of the disordered $\langle A_{0.5}B_{0.5}\rangle C$ alloy in three conceptual steps.

First, neglecting both structural relaxations (i.e., by using $u = \frac{1}{4}$, $\eta = 1$) and the ordering potential $\Delta V = V_T - V_{ZB}$, the bands of ABC_2 could be obtained from those of the virtual $\langle A_{0.5}B_{0.5}\rangle C$ crystal by folding the latter into the tetragonal Brillouin zone of ABC_2. The folding relations are[10] $\bar{\Gamma} \leftrightarrow \tilde{\Gamma} + \tilde{X}_z$, $\bar{M} \leftrightarrow \tilde{X}_x + \tilde{X}_y$, and $\bar{R} \leftrightarrow \tilde{L} + \tilde{L}$, where x, y, and z denote directions parallel to the cell axes a, b, and c. This mapping creates extra degeneracies at $\bar{M}$ and $\bar{R}$ [formed by folding two *equivalent* ZB states] and renders the indirect ZB state $\tilde{X}_c$ "pseudodirect" (i.e., folded into $\bar{\Gamma}$), but does not shift the band energies.

Second, turn on the ordering potential $\Delta V(\mathbf{r})$, still keeping ABC_2 unrelaxed. This potential now distinguishes the A and B sublattices. For *common-cation* compounds the roles of $\tilde{X}_1$ and $\tilde{X}_3$ are interchanged.[11] The three main effects of ΔV are the following: (i) States of ordered ABC_2 with the same symmetry can interact through ΔV, hence repel each other. This is the case for the pairs $\{\bar{\Gamma}_{1v}(\tilde{X}_{3v});\bar{\Gamma}_{1v}(\tilde{\Gamma}_{1v})\}$, $\{\bar{\Gamma}_{1c}(\tilde{X}_{3c});\bar{\Gamma}_{1c}(\tilde{\Gamma}_{1c}\}$, and $\{\bar{\Gamma}_{5v}(\tilde{X}_{5v});\bar{\Gamma}_{5v}(\tilde{\Gamma}_{15v})\}$ in the common-anion alloys,[11] where we indicated in parentheses the zinc-blende states folded into the superlattice state. (ii) Degeneracies present in the first step will be removed, e.g., between the pairs $\{\bar{R}_{1c}(\tilde{L}_{1c});\bar{R}_{4c}(\tilde{L}_{1c})\}$, $\{\bar{M}_{2c}(\tilde{X}_{3c});\bar{M}_{1c}(\tilde{X}_{3c})\}$, and $\{\bar{\Gamma}_{5v}(\tilde{\Gamma}_{15v});\bar{\Gamma}_{4v}(\tilde{\Gamma}_{15v})\}$, introducing new pseudodirect transitions (Fig. 1). The angular momentum character of the random alloy states will be altered, thereby changing the spin-orbit splitting [which increases (decreases) with $p(d)$ character]. For example, the $\tilde{\Gamma}_{15v}$ valence band maximum (a non-s state in zinc-blende symmetry) can acquire some s characer in $\bar{\Gamma}_{4v}$, whereas the $\tilde{\Gamma}_{1c}$ state (a non-p state in zinc-blende symmetry) can acquire p and d character in $\bar{\Gamma}_{1c}$.

In the *third*, final step of our conceptual transformation

TABLE I. Difference (in eV) between the average band energies of the binary constituents and the corresponding states (see Fig. 1) of the ordered ABC_2 phase in the CuAuI-like $(AC)_1(BC)_1$ (001) superlattice structure. The zero of energy is set at the $\bar{\Gamma}_{5v}(\tilde{\Gamma}_{15v})$ valence band maximum. The labels of the $\tilde{X}$ points take the origin on the anion site: $\alpha = 1, \beta = 3$ for common-anion compounds and $\alpha = 3, \beta = 1$ for common-cation compounds (see Ref. 11). The values of u are given in the headings.

u	ZnS ZnSe 0.237	ZnSe ZnTe 0.230	ZnS ZnTe 0.217	HgTe CdTe 0.250	CdTe ZnTe 0.227	HgTe ZnTe 0.227	GaAs AlAs 0.246	GaAs GaSb 0.234
$\tilde{\Gamma}_{15c} - \bar{\Gamma}_{5c}$	0.04	0.12	0.29	0.00	−0.02	−0.02	0.01	0.09
$\tilde{\Gamma}_{15c} - \bar{\Gamma}_{4c}$	0.03	0.14	0.31	0.00	−0.02	−0.02	0.02	0.07
$\tilde{X}_{\beta c} - \bar{\Gamma}_{1c}$	−0.03	−0.31	−0.43	−0.03	0.08	0.07	−0.24	−0.18
$\tilde{X}_{\beta c} - \bar{M}_{2c}$	0.60	0.12	0.15	−0.37	−0.34	−0.74	−0.38	0.18
$\tilde{X}_{\beta c} - \bar{M}_{1c}$	0.99	0.16	0.53	0.37	0.33	0.79	0.39	0.02
$\tilde{X}_{\alpha c} - \bar{\Gamma}_{4c}$	0.07	0.17	0.43	0.00	−0.08	−0.15	−0.02	0.16
$\tilde{X}_{\alpha c} - \bar{M}_{5c}$	−0.69	0.16	0.39	0.00	0.01	0.02	0.01	0.11
$\tilde{L}_{1c} - \bar{R}_{4c}$	−0.14	−0.49	−0.49	−0.36	−0.01	−0.25	−0.48	−0.35
$\tilde{L}_{1c} - \bar{R}_{1c}$	0.23	0.70	1.10	0.38	0.13	0.43	0.47	0.53
$\tilde{\Gamma}_{1c} - \bar{\Gamma}_{1c}$	0.10	0.49	0.95	0.01	0.11	0.11	0.20	0.30
$\tilde{\Gamma}_{15v} - \bar{\Gamma}_{5v}$	0.00	0.00	0.00	0.00	0.00	0.00	0.00	0.00
$\tilde{\Gamma}_{15v} - \bar{\Gamma}_{4v}$	0.06	0.14	0.37	0.01	0.13	0.23	0.05	0.09
$\tilde{X}_{\beta v} - \bar{\Gamma}_{1v}$	0.02	−0.52	−0.44	0.04	−0.01	0.06	0.00	0.00
$\tilde{\Gamma}_{1v} - \bar{\Gamma}_{1v}$	0.05	0.76	1.01	0.02	0.03	0.04	0.03	0.24

of the disordered alloy into ordered ABC_2, we permit the atomic structure to relax, i.e., we replace the unrelaxed parameters ($u = \frac{1}{4}, \eta = 1$) by their equilibrium values (calculated, e.g., in Ref. 10). Quantitative calculations[12] of the band structure of ABC_2 as a function of u and η show that relaxation of u lowers $\bar{\Gamma}$ gap further, relative to $u = \frac{1}{4}$, and that an increase in η beyond 1.0 pushes[13] the $\tilde{X}$-derived states $\bar{M}_{5c}$, $\bar{M}_{1c}$, and $\bar{M}_{2c}$ to *lower* energies relative to $\bar{\Gamma}_{1c}(\tilde{X}_3)$.

To assess *quantitatively* the effects of the formation of ordered structures on the band structure we have carried out first-principles self-consistent local density band structure calculations on a series of $\{AC, BC, ABC_2\}$ isovalent semiconductors.[14] The calculations on ABC_2 were performed at the average lattice constant of AC and BC; the values of u and η were obtained by finding those values which minimize the elastic energy, i.e., best accommodate the dissimilar AC and BC bonds[12] (Table I). The values of η were, in all cases, very close to 1.000. Figure 1 depicts the mapping of the averages of the states of the binary compounds into those of the CuAuI-like ordered *common-anion* ABC_2 compound. In Table I we compare the *shifts* between the average calculated energies of AC and BC with the corresponding calculated energies in ABC_2 (see Fig. 1 for the level correspondences). While such shifts in actual samples will depend sensitively on the *degree* of order attained (which, in turn, depends on growth conditions), we discuss here the ordering-induced changes in the limit of *perfect* ordering, i.e., without disorder broadening:

(i) The conduction band state $\bar{\Gamma}_{1c}$ of the superlattice shifts *downward* upon ordering (reducing the $\bar{\Gamma}_{15v} \rightarrow \bar{\Gamma}_{1c}$, or "$E_0$ gap" relative to the average energy) by an amount in-

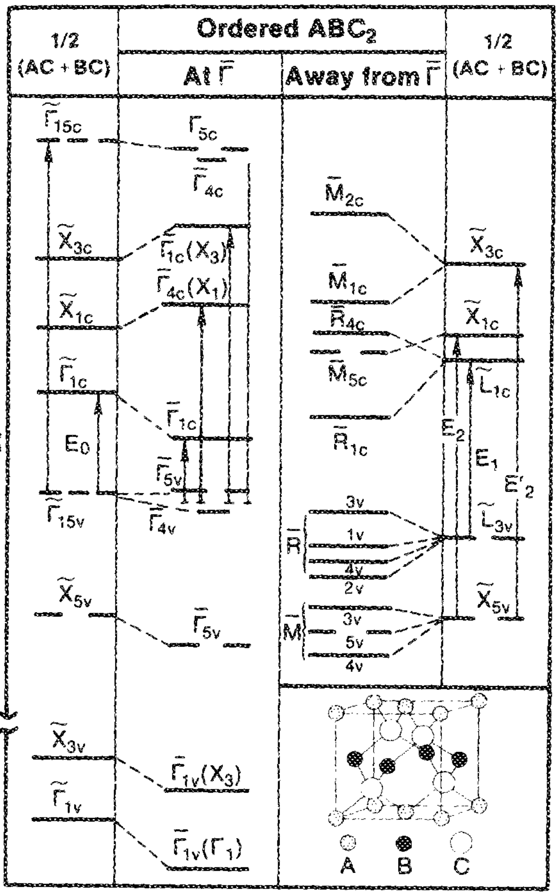

FIG. 1. Relationship between the states of the random alloy $(A_{0.5}B_{0.5})C$ in the virtual crystal model and the corresponding states of an ordered *common-anion* compound ABC_2 in the CuAuI-like structure.

versely proportional to the $\tilde{X}_{3c} - \tilde{\Gamma}_{1c}$ or $\tilde{X}_{1c} - \tilde{\Gamma}_{1c}$ energy difference[11] [as large as 1.3–2.5 eV in ZnS-ZnSe and HgTe-CdTe, but only 0.8 eV in ZnS-ZnTe and directly proportional to the disparity between the mixed atoms (small for Ga-Al or Hg-Cd, having similar sizes and electronegativities)].

(ii) New pseudo*direct* transitions (indirect in the disordered alloy) appear, e.g., $\bar{\Gamma}_v \to \bar{\Gamma}_{4c}(\tilde{X}_{1c})$ and $\bar{\Gamma}_v \to \bar{\Gamma}_{1c}(\tilde{X}_{3c})$. While weaker than truly direct transitions [e.g., $\bar{\Gamma}_v \to \bar{\Gamma}_{1c}(\tilde{\Gamma}_{1c})$], coupling through $\Delta V \neq 0$ and atomic relaxations makes these transitions considerably more intense than truly indirect (e.g., $\tilde{\Gamma}_v \to \tilde{X}_c$) transitions. Relative to the average $\tilde{\Gamma}_v \to \tilde{X}_{1c}$ transition, $\bar{\Gamma}_v \to \bar{\Gamma}_{4c}$ is shifted mostly to *lower* energies in mixed-anion systems and to *higher* energies in mixed-cation systems.

(iii) The valence band maximum in the alloy ($\tilde{\Gamma}_{15v}$ in the absence of spin-orbit splitting, $\tilde{\Gamma}_{8v} + \tilde{\Gamma}_{7v}$ with spin-orbit) splits in ordered ABC_2 to $\bar{\Gamma}_{4v} + \bar{\Gamma}_{5v}$; since these are anion-like states, the splitting is larger in mixed-anion than in mixed-cation systems. $\bar{\Gamma}_{5v}$ moves to higher energies because of repulsion by $\bar{\Gamma}_{5v}(\tilde{X}_{5v})$ below it. These $\bar{\Gamma}_{5v} + \bar{\Gamma}_{4v}$ (crystal-field split) states can couple through spin-orbit interactions, giving rise to a total of three states (instead of just two in the random alloy or the binaries). The upper two ($\bar{\Gamma}_{7v} + \bar{\Gamma}_{6v}$) evolve mostly from the alloy $\tilde{\Gamma}_{8v}$, and their small separation (calculated to be 90, 130, and 10 meV for ZnCdTe$_2$, ZnHgTe$_2$, and CdHgTe$_2$, respectively) is proportional to the crystal field splitting. A smaller splitting is apparent in the more extended $\tilde{\Gamma}_{15c}$ conduction band.

(iv) The $\tilde{L}_{1c}$ conduction band state splits into the $\bar{R}_{1c} - \bar{R}_{4c}$ pair in ABC_2. Since one samples the perturbation $V_{A,s} - V_{B,p}$ and the other samples $V_{B,s} - V_{A,p}$, the $\bar{R}_{1c} - \bar{R}_{4c}$ splitting can be very large. In fact, we find that the energies of $\bar{R}_{1c}$ and $\bar{R}_{4c}$ are closer to the energies of the corresponding L_{1c} states *of the pure binary constituents rather than to their average.* This dramatic splitting should be observed in E_1-derived modulated reflectance spectroscopy (observe that the initial $\tilde{L}_{3v}$ state is also split into four components; see Fig. 1). In GaAlAs$_2$ the splitting is so large that the lower $\bar{R}_{1c}$ state is below $\bar{\Gamma}_{1c}$ and $\bar{M}_{5c}$, making the system *indirect* at $\bar{R}_1(\tilde{L})$. Evidence for this effect was recently found in reflectance spectra[15] of (GaAs)$_1$(AlAs)$_1$: the $\bar{R}_v \to \bar{R}_{1c}$ transition observed at 3.2 eV is lower by $\simeq 0.3$ eV (calculated: 0.47 eV) than the average of the $L_{3v} \to L_{1c}$ transitions in GaAs (3 eV) and AlAs (4 eV). A similarly large splitting of $\tilde{X}_{3c}$ (into $\bar{M}_{1c} + \bar{M}_{2c}$) should be observable in the $\tilde{X}_{5v} \to \tilde{X}_{3c}(E_2)$ spectra. These splittings are so large that we expect them to partially survive disorder and constitute a sensitive test of partial ordering of the alloy.

(v) In both common-anion and common-cation compounds the $\tilde{X}$ state nearest the valence band minimum $\tilde{\Gamma}_{1v}$ is of $\tilde{X}_{1v}$-type (*pd* on cation, *sd* on anion, using the origin on the anion site). However, only in *common-cation* compounds does this state fold into $\bar{\Gamma}_{1v}(\tilde{X}_{1v})$, hence repelling $\bar{\Gamma}_{1v}(\tilde{\Gamma}_{1v})$. Since in these common-cation compounds the energy difference $\tilde{X}_{1v} - \tilde{\Gamma}_{1v}$ is generally small (~ 1 eV[10]), the repulsion upon formation of ordered ABC_2 (given by the difference of the $\tilde{\Gamma}_{1v} - \bar{\Gamma}_{1v}$ and $\tilde{X}_{1v} - \bar{\Gamma}_{1v}$ energy differences in Table I, e.g., $1.01 + 0.44 = 1.45$ eV for ZnS-ZnTe) is found to be large and should be observable in photoemission. In contrast, in *common-anion* compounds we expect a smaller effect, since it is the state $\tilde{X}_{3v}$ (*sd* on cation, *pd* on anion) that folds into $\bar{\Gamma}_{1v}$ and $\tilde{X}_{3v}$ is considerably higher than $\tilde{\Gamma}_{1v}$ (by $\sim$6–7 eV). Hence it is predicted to have only a small repulsion (e.g., $0.04–0.02 = 0.02$ eV in HgCdTe$_2$).

Table I and Fig. 1 can be used to estimate the conduction band energies of an ordered (001) monolayer superlattice, given the energies of the binaries. For example, the average of the experimental (low temperature) Γ_{1c} energies of GaAs and AlAs is $(1.52 + 3.13)/2 = 2.325$ eV. Table I and Fig. 1 show that $\bar{\Gamma}_{1c}(\tilde{\Gamma}_{1c})$ of the superlattice is lower than the corresponding averages of the binary systems by 0.20 eV, predicting $\bar{\Gamma}_{1c}(\tilde{\Gamma}_{1c})$ at $2.325–0.20 = 2.13$ eV. The corresponding energies of the Ga$_{0.5}$Al$_{0.5}$As alloy can be obtained from the average energies of the binaries, corrected by the measured bowing parameter ($b_\Gamma = 0.37$ eV).[15] This gives a 0 K Γ_{1c} at 2.23 eV. Hence we predict that the superlattice $\bar{\Gamma}_v \to \bar{\Gamma}_{1c}(E_0)$ transition will be 0.1 eV below the alloy and 0.2 eV below the binary-averaged transitions. Experimentally, indeed the superlattice E_0 transition is at $\sim$2.15 eV,[15] whereas the alloy E_0 (extrapolated to 0 K) is at $\sim$2.23 eV.

---

[1] M. B. Panish and M. Ilegems, Prog. Solid State Chem. **7**, 39 (1972); G. B. Stringfellow, J. Cryst. Growth **27**, 21 (1974).

[2] M. Jaros, Rep. Prog. Phys. **48**, 1091 (1985).

[3] D. Long, in *Semiconductors and Semimetals*, edited by R. K. Willardson and A. C. Beer (Academic, New York, 1966), Vol. 1, p. 143.

[4] G. P. Srivastava, J. L. Martins, and A. Zunger, Phys. Rev. B **31**, 2561 (1985); J. L. Martins and A. Zunger, J. Mater. Res. **1**, 523 (1986); A. Mbaye, L. G. Ferreira, and A. Zunger, Phys. Rev. Lett. **58**, 49 (1987); A. Zunger, Int. J. Quantum Chem. **19**, 629 (1986); A. Zunger, Appl. Phys. Lett. **50**, 164 (1987).

[5] H. Nakayama and H. Fujita, in *GaAs and Related Compounds 1985*, Karuizawa, Japan, edited by M. Fujimoto (Hilger, Bristol, 1986), p. 289.

[6] (a) T. S. Kuan, W. J. Wang, and E. L. Wilkie, Appl. Phys. Lett. **51**, 51 (1987). (b) M. A. Shahid, S. Mahajan, D. E. Laughlin, and H. M. Cox, Phys. Rev. Lett. **58**, 2567 (1987).

[7] H. R. Jen, M. J. Cherng, and G. B. Stringfellow, Appl. Phys. Lett. **48**, 1603 (1986).

[8] A. Gomyo, T. Suzuki, K. Kobayashi, S. Kawata, and I. Hino, Appl. Phys. Lett. **50**, 673 (1987).

[9] T. S. Kuan, T. F. Kuech, W. I. Wang, and E. L. Wilkie, Phys. Rev. Lett. **54**, 201 (1985).

[10] J. E. Bernard and A. Zunger, Phys. Rev. B **34**, 5992 (1986); **36**, 3199 (1987).

[11] We place the origin of the coordinate system on the anion site. The nondegenerate zinc-blende or alloy state at X with *sd* character on the anion and *pd* character on the cation is labeled $\tilde{X}_1$, whereas the state with *pd* character on the anion and *sd* character on the cation is labeled $\tilde{X}_3$. In common-cation (anion) ABC_2 compounds $\tilde{X}_1$ maps into $\bar{\Gamma}_1 + \bar{M}_1 + \bar{M}_2$ ($\bar{\Gamma}_4 + \bar{M}_5$), whereas $\tilde{X}_3$ maps into $\bar{\Gamma}_4 + \bar{M}_5$ ($\bar{\Gamma}_1 + \bar{M}_1 + \bar{M}_2$) (see Table I).

[12] A. Zunger and J. Jaffe, Phys. Rev. Lett. **51**, 662 (1983); J. Jaffe and A. Zunger, Phys. Rev. B **29**, 1882 (1984).

[13] T. P. Pearsall, F. H. Pollak, J. C. Bean, and R. Hull, Phys. Rev. B **33**, 6821 (1986).

[14] For ZnS-ZnSe, ZnSe-ZnTe, and ZnS-ZnTe, we have used the all-electron potential-variaton mixed-basis method (Ref. 10); for Hg, Zn, and Cd tellurides, and GaAs-GaSb, we have used the linear augmented plane wave method [S.-H. Wei and H. Krakauer, Phys. Rev. Lett. **55**, 1200 (1985)]; and for GaAs-AlAs we have used the nonlocal pseudopotential method [D. M. Wood, S.-H. Wei, and A. Zunger, Phys. Rev. Lett. **58**, 1123 (1987)]. In the latter reference and in Ref. 10 we compare the results of these methods for two systems (GaAs and ZnTe) and find differences in band energies not to exceed 0.1–0.2 eV.

[15] M. Cardona, T. Suemoto, N. E. Christensen, T. Isu, and K. Ploog, Phys. Rev. B **36**, 5906 (1987); H. J. Lee, L. Y. Juravel, J. C. Woolley, and A. J. Spring Thorpe, Phys. Rev. B **21**, 659 (1980).